ISSN (e): 2250 – 3005 || Volume, 08 || Issue, 4|| April – 2018 ||
International Journal of Computational Engineering Research (IJCER)

Effects of coal seam dip angle on the outburst in coal roadway excavation

Tapan Kumr Mohanty [1] Niraj Kumar [2] Anil Panda [3] Dr. B. S. Patra[4]
Department of Mechanical Engineering,Aryan Institute of Engineering & Technology, Bhubaneswar
Department of Mechanical Engineering, Raajdhani Engineering College, Bhubaneswar
Department of Mechanical Engineering, Capital Engineering College, Bhubaneswar
Department of Mechanical Engineering, NM Institute of Engineering & Technology, Bhubaneswar

Abstract
The prevention and forecast of coal and gas outburst has always been one of the key issues in coal mining safety. By simulating the process of tunneling in coal seam with different dip angle through FLAC3D soft- ware, the dangerous zone in which outburst may occur and the probability of outburst near the working face were predicted through the distribution of stress, displacement and plastic zone. Then we discussed the size of unstable area in the surrounding rock through the distribution of stress and the variation curve of the displacement on the roadway wall. The results show that, with an increase of the coal seam dip angle, the risk of outburst in the working face rises gradually. And the dangerous areas in which may out- burst occur moves to the upper part of coal seam. The size of unstable area in the surrounding rock increases with the increase of coal seam dip angle

I. INTRODUCTION

Every coal mine accident may cause a large number of casualties, property losses and environmental damage, in which coal and gas outburst is the most serious one [1–3]. And with the continuous increase of mining depth in coal mines, the threat of coal and gas outburst accidents becomes more and more serious [4–6]. So the prevention and forecast of coal and gas outburst has always been one of the key issues in coal safety.

Many experts had done a lot of research on it, Ou et al. [7–9] studied the instability mechanism of gas outburst; Du et al. [10] analyzed the variation correlation between prediction index of coal and gas outburst and tunneling speed; Zhang et al. [11] believed that engineering factors play a leading role in coal and gas out- burst. However, coal and gas outburst is extremely difficult to be predicted and prevented [12,13]. The mechanism of coal and gas outburst has not been found fully up to now [14–16].

In order to predict and prevent gas outburst, Liu et al. [17–20] put forward suggestions on gas outburst from safety supervision, work management and other aspects. Researches show that hydraulic technologies, such as hydraulic fracturing [21–23], coalflooding [1,24–27], hydraulic cutting [28–30], hydraulic punching [31–33], can be used to reduce the risk of coal and gas outburst. Wang et al. [34] established the electromagnetic radiation warning criteria for coal and gas outbursts. Jiang et al.
[35] proposed a real-time monitoring and early warning method for coal and gas outburst.

As a powerful numerical simulation software, FLAC3D is very suitable for large-scale numerical simulation. Shu et al. [36] used FLAC3D to calculate and analyze the distribution characteristics of mining stress and failure zone of working face under various conditions, then the main controlling factors and influencing mechanism of outburst danger in coal driving are studied. Guo et al. [37] used FLAC3D to compare and analyze the deformation law of surrounding rock under different support schemes, and chose the best support mode for different coal mine. Through numerical simulation, Li et al. [38,39] studied the influence of in- situ stress and roadway layout on the coal seam gas extraction and the mechanical characteristics of roadway. Yang [40] estab- lished a stope spatial distribution model and a safe and efficient mining model for coal seams with FLAC3D. And then he solved the technical problems of pressure relief gas control in close- distance and long-distance coal seam group.
All the above studies can explain the mechanism of gas outburst from some aspects, and reduce the risk of gas outburst to a certain extent. But there are few studies on the effect of coal seam dip angle on gas outburst.

In order to solve these problems, it is necessary to explore the effect of coal seam dip angle on gas outburst. The objective of this work was to quantitatively evaluate the effect of coal seam dip angle on gas outburst through FLAC3D numerical simulation.

II. MODEL ESTABLISHMENT

Rigorous investigation of coal tunneling with different coal seam dip can be a difficult task due to several complicating factors:

(1) it is almost impossible to find a group of coal seams with differ- ent dip angles, but with the same mechanical and physical proper- ties [41]; (2) the presence of materials (coal and rock mass) with distinct mechanical properties [1]; and (3) the anisotropy of the in situ stress in the ground [38]. To reproduce accurately the effects of the dip angle on coal roadway excavation, the analysis cannot be treated as a two-dimensional (2D) problem using plane strain or axisymmetric analysis but requires the use of three-dimensional (3D) modeling [40]. As a 3D explicit finite-difference program, FLAC3D is suitable to solve the above problems. Therefore, FLAC3D was used in the study to perform numerical analyses.

In this study, seven simulation models of tunneling in coal seam with coal seam dip angle being 0°, 5°, 10°, 15°, 20°, 25° and 30° respectively, were established by the simulation software FLAC3D. The ground stress of the model was set as 20 MPa according to the

measured ground stress in the Pingdingshan Coal Mine, and the mechanical parameters of coal seam are listed in Table 1. The model, divided into three layers, was in a size of 80 m 80 m 80 m.

× × The middle layer of the model is coal seam. The upper and lower layers of the model are rock layers, which are the roof and floor of coal seam respectively. The thickness of the coal seam is 4.2 m. The roadway was drilling in the middle of the coal seam, and the road- way was 5 m wide with a height of 3.2 m in the center of the roadway.

The mechanical constitutive model used in the model was Mohr-Coulomb criterion. Roller boundaries were used for the ini- tial response along the sides and bottom of the model. The ground stress 20 MPa was applied at the top of the model. 61 measuring points were arranged along the direction perpendicular to the roadway, the distance between adjacent measuring points was 1 m. The measured points can record the changes of stress and dis- placement in real time. The boundary conditions, element types, and mesh density of the model were selected based on several sen- sitivity analyses to eliminate their influence on the results. Numer- ical model with a dip angle of 20° is shown in Fig. 1.

III. EFFECT OF COAL SEAM DIP ANGLE ON OUTBURST OF DRIVING FACE

Stress analysis of driving face

Fig. 2 shows the maximum principal stress nephogram of driv- ing face. The red area in the figure represents the part with small stress, while the blue area represents the part with large stress. It can be seen from the figure that stress concentration areas exist in the coal seam on the two sides of the driving face. And the stress in the part of the driving face is very small because the surrounding coal and rock is affected by mining, which causes loosening and is not easy to carry out stress concentration. The distance between the stress concentration area and the roadway wall, as well as the maximum stress value, under different coal seam dip angle are recorded and plotted as Fig. 3. As can be seen from Fig. 3, the distance between the stress concentration area in the upper side of roadway and the roadway wall increases gradually while the

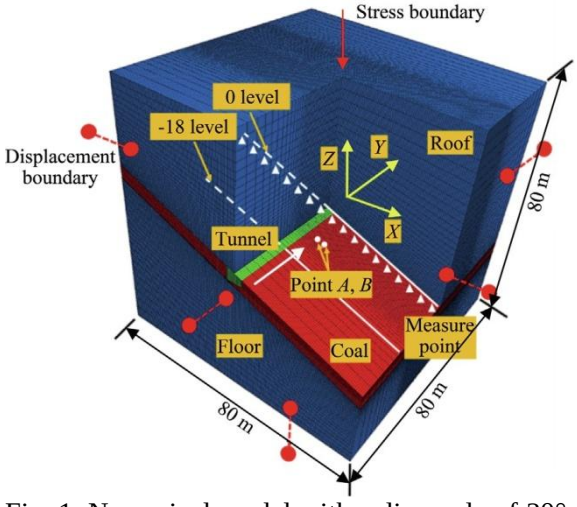

Fig. 1. Numerical model with a dip angle of 20°.

distance between stress concentration area in the lower side decreases gradually with the rise of coal seam dip angle. That is to say, the stress concentration areas in the coal seam around the roadway show a trend of migration along the coal seam to the upper side of roadway.

With the rise of coal seam dip angle, the maximum stress in the driving face increases gradually from 29.87 MPa to 31.27 MPa, with an increase of about 4.7%, which means that the risk of out- burst around the roadway goes up as well.

Fig. 4 shows the curves of maximum principal stress of two measuring points (*A* and *B*), which are 6 m and 8 m away from the roadway wall in the driving process, respectively. The location choosing of the two measurement points *A* and *B* is because the stress concentration area in the coal seam is about 5–10 m away from the roadway wall. The abscissa in Fig. 4 represents the dis- tance between the section of heading face and the measuring point, and the negative value indicates the distance of driving after the heading face exceeds from the measuring point. As can be seen from Fig. 4, the stress at the measuring point goes up gradually at first and then drops dramatically at a certain point with the driving of coal roadway. This is because when the coal roadway drives near the measuring point, the stress balance around the point was destroyed. The comparison of stress curves under different coal seam dip angle indicates that the greater the coal seam dip angle is, the later the stress at the measuring point begins to decline, and the greater the maximum stress will be. This also proves that the greater the dip angle of coal seam is, the greater the outburst risk is.

Displacement analysis of driving face

In the process of roadway excavation, the original stress state of coal seam is destroyed, and a certain degree of displacement often occurs in the coal seam. If the displacement of a part is too large, the danger of outburst will be great, so the analysis of displace- ment around the heading head is also an effective method to judge the danger of outburst.

Table 1
Mechanical parameters of coal and rock.

Group	Modulus (GPa)	Poisson ratio	Friction angle (°)	Cohesion (MPa)	Density (kg/m^3)
Coal	2	0.35	20	0.3	1350
Rock	10	0.3	25	2	2500

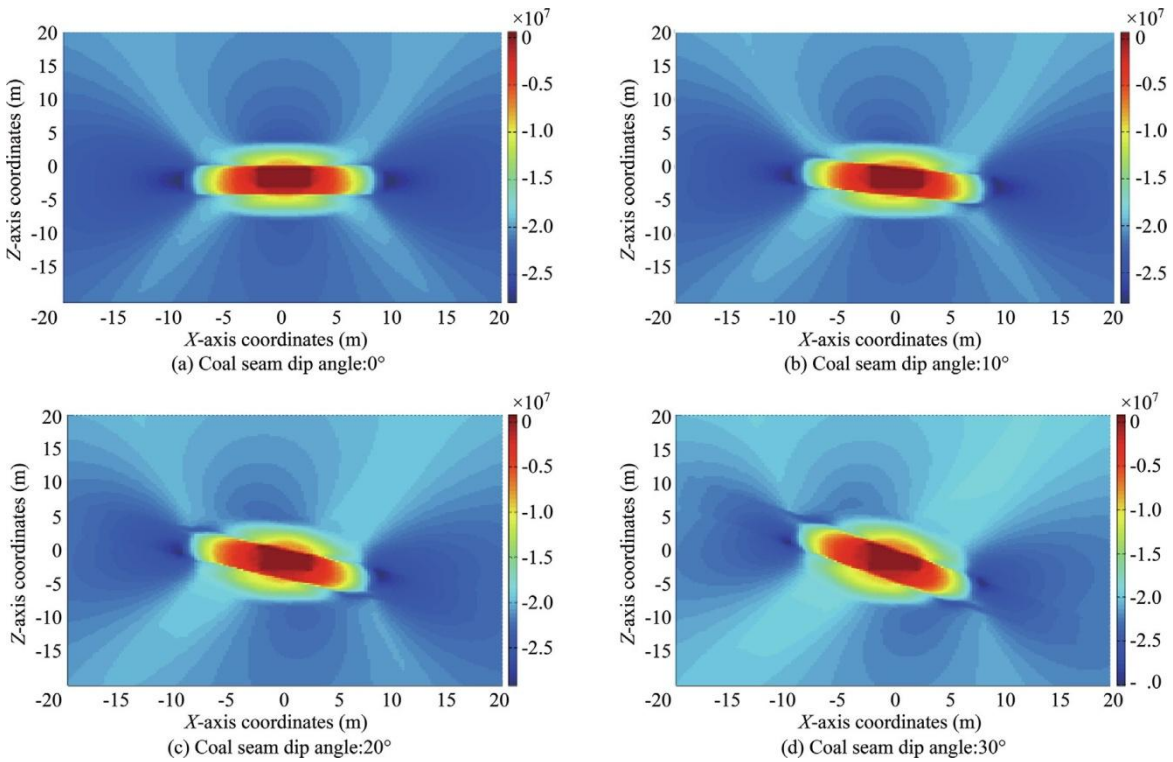

Fig. 2. Nephogram of maximum principal stress in driving face.

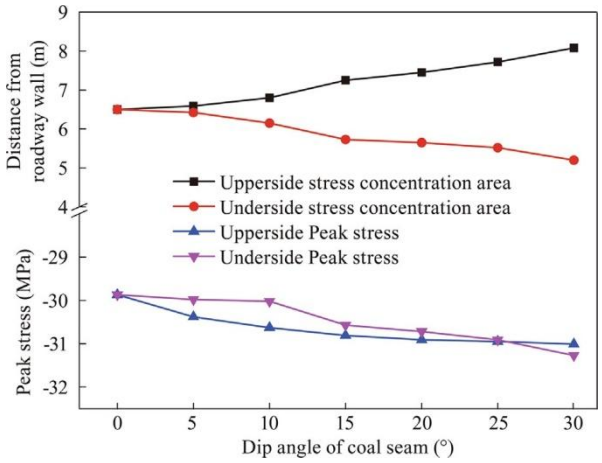

Fig. 3. Statistical chart of dates in stress concentration area.

Fig. 5 exhibits the displacement nephogram of driving face pro- file, from which it can be seen that the large displacement area around the roadway is mainly concentrated in the coal seam near the roadway floor and the roadway walls, but the displacement of rock layer is very small. With the rise of coal seam dip angle, the total area of large displacement area around the roadway gradually increases, and so does the large displacement area near the upper side of roadway and the floor. On the contrary, the large displace- ment area near the lower side of roadway gradually decreases.

The range of large displacement area can reflect the location of outburst, and the maximum displacement can reflect the probabil- ity of outburst. By observing the displacement nephogram under different coal seam dip angle and comparing its maximum displace- ment, we can find that the maximum displacement increases with the increase of coal seam dip angle, but the increment of displacement is not obvious. When the dip angle of coal seam is 0°, the maximum displacement is 15.08 cm, while the dip angle of coal seam increases to 30°, the maximum displacement increases to 15.25 cm, which increases only 0.17 cm. That is to say, the change of coal seam dip angle has some influence on the maximum displacement around the roadway, but the effect is not obvious.

Fig. 6 is the displacement curves of seven groups of measuring points near the upper side of roadway. It can be seen from the observation of single curve that the displacement of coal seam declines gradually, and the extent of its decline decreases gradually with the increase of the distance from the roadway wall. When the distance from the roadway exceeds a certain number, the displace- ment tends to be stable. This is because roadway excavation mainly affects the coal seam around the roadway, so the displace- ment of the coal seam near the roadway wall is always greater than that of other areas. As the distance from the roadway increases gradually, the influence of excavation decreases, and the displace- ment tends to be stable.

It can be seen from the comparison of the displacement curves under different coal seam dips that the displacement curves of coal seams show a gradual upward trend with the increase of coal seam dips, which means the displacement in coal seams has been gener- ally increased.

Through the displacement analysis of driving face, it can be found that the displacement of coal seam generally increases with the rise of coal seam dip angle, and the probability of outburst goes up. Meanwhile, the large displacement area gradually migrates to the upper side of roadway, and the outburst- prone area focuses on the upper side of roadway and the floor.

Plastic zone analysis of driving face

Most materials have an elastic limit, when the stress is less than the elastic limit, the material is in the state of elastic deformation. Although deformation can also occurs in the materials under the

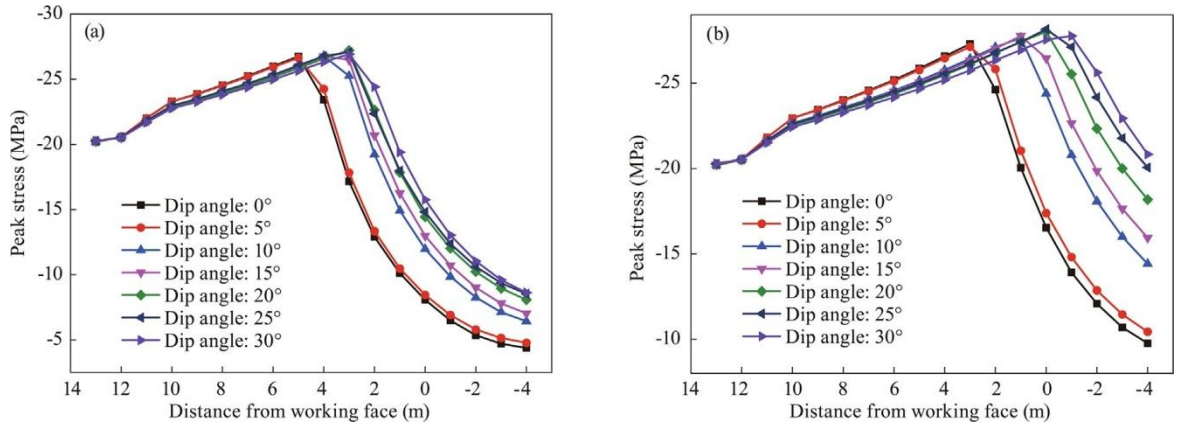

Fig. 4. Stress curve of measuring points.

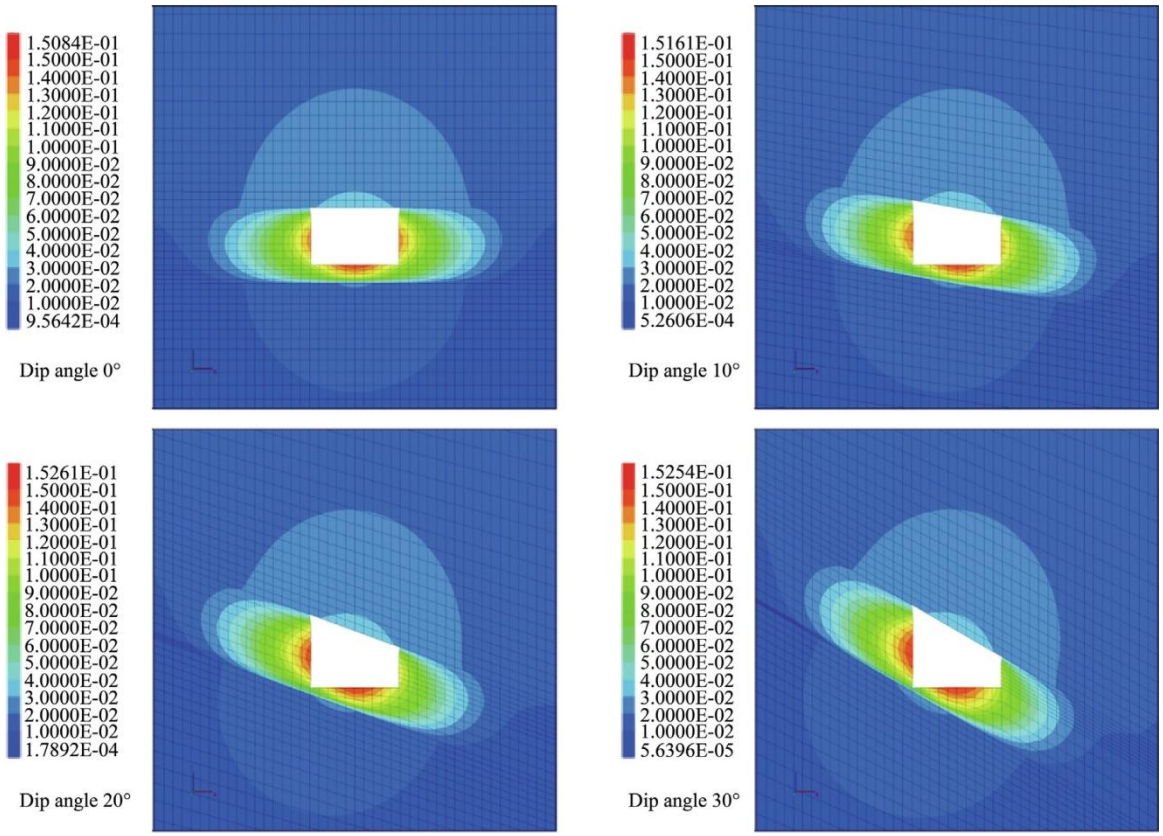

Fig. 5. Displacement nephogram in heading face.

state of elastic deformation, the materials will restore to its original shape once the stress is removed. When the stress on the material exceeds the elastic limit, the material is in a plastic state. The deformation of material in plastic state cannot be completely restored even if the stress is removed.

There are also elastic limit and plastic state in coal. The coal area in the plastic state is called plastic zone, which is the area with high stress, large deformation and is prone to occur outburst. Therefore, statistical analysis of the plastic zone around coal road- way is also an effective means to predict the location and risk of outburst.

The plastic zone nephograms of coal seam profile and driving face profile are displayed in Figs. 7 and 8. The blue, green and red zones represent the non-plastic zone, the original plastic zone and the plastic zone, respectively. Non-plastic zone is mainly located in the coal and rock seam far away from the roadway, which belongs to the safe area with small stress, small deformation and small risk of outburst. Original plastic zone is the area which has been in a plastic state, but it has restored to an elastic state when stress has been withdrawn. This is because in the early stage of roadway excavation, the stress balance of coal and rock around the roadway is suddenly destroyed, resulting in a large number of stress concentration, which makes the stress of coal and rock around the roadway quickly reach the elastic limit.

Then the stress induces the deformation of coal seam, and the stress is decom- posed and transferred at the same time. When the coal seam

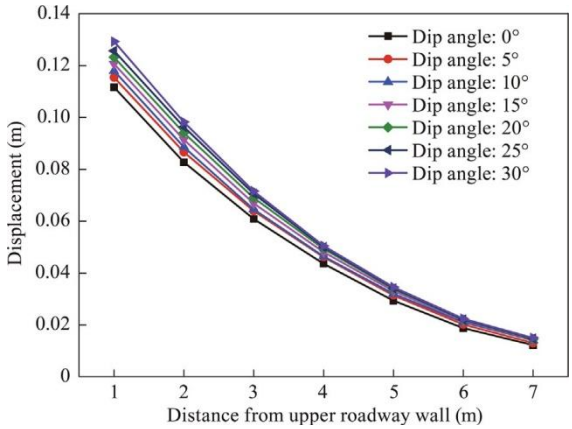

Fig. 6. Displacement curve of measuring points.

reaches the stress balance again, the stress value of most coal and rock areas decreases greatly and recovers from the plastic state to the elastic state. This kind of area distributes evenly in the coal and rock seam around the roadway, but the range of distribution in the coal seam is slightly larger than that in the rock seam. Although the stress in this kind of region is relatively small temporarily, the elas- tic limit of the material after entering the plastic state decreases, so it is easier for this region to re-enter the plastic state, which makes it belongs to the warning area that needs attention. Plastic zone is the area where the stress of coal and rock is still in plastic state after equilibrium is destroyed and rebalanced. This area mainly distributes in the coal seam around the roadway, and hardly exists in the rock seam. Plastic zone is the dangerous area with concen- trated stress, large deformation and high risk of outburst around roadway.

It can be seen from Fig. 7 that the surrounding rock of roadway relatively far from the working face is basically in a plastic state and is less affected by the dip angle of coal seam. However, affected by the dip angle of coal seam, the coal seam near the working face exhibits more obvious plastic state.

As presented in Fig. 8, the ranges of non-plastic zone and orig- inal plastic zone rarely vary with coal seam dip angle, while that of plastic zone is significantly affected by coal seam dip angle.

Firstly, in terms of area, when the dip angle of coal seam is 0°, the plastic zone is scattered around the roadway, and the area of the plastic zone in coal seam is less than 5% of the total area of the original plastic zone and the plastic zone. With the increase of coal seam dip, the original plastic zone gradually transforms into plastic zone. When the dip angle of coal seam increases to 25°, the area of plastic zone in coal seam is almost 50% of the total area of original plastic zone and plastic zone.

Then from the position of the plastic zone, it is observed that when the dip angle of the coal seam is 0°, the plastic zone disperses around the roadway. With the increase of coal seam dip, the plastic zone gradually gathers to the upper side of coal and floor. When the coal seam dip is 25°, the upper half of the upper coal seam and the floor area of the roadway are all in plastic state.

This indicates that the risk of outburst in roadway driving face increases gradually with the rise of coal seam dip angle, and the dangerous area moves to the upper side of roadway gradually.

IV. EFFECT OF COAL SEAM DIP ANGLE ON UNSTABLE ZONE OFROADWAY SURROUNDING ROCK

Affected by coal roadway driving, the surrounding rock of road- way is prone to the outburst accident because the original stress balance is destroyed. However, with the increase of distance from the heading face, the surrounding rock gradually restores balance. By comparing the unstable state of surrounding rock under differ- ent coal seam dip angle, the influence of coal seam dip angle on the unstable area of surrounding rock can be obtained.

Stress analysis of roadway surrounding rock

Fig. 9 is a maximum principal stress nephogram of coal seam profile, it can be seen from Fig. 9 that the stress nephograms under different coal seam dip angle present a ‘‘weak-strong-weak” semi-elliptic distribution from the roadway outward.

Draw a straight line at the heading face along the coal seam and mark it as the 0 horizontal line, and the 0

horizontal line is perpen- dicular to the roadway. Then another 6 straight lines parallel to 0 horizontal line were made every 3 m from the heading face down to the internal roadway, and the lines were marked as —3, —6, —9,
—12, —15, —18 horizontal lines. A total of 61 sets of measuring

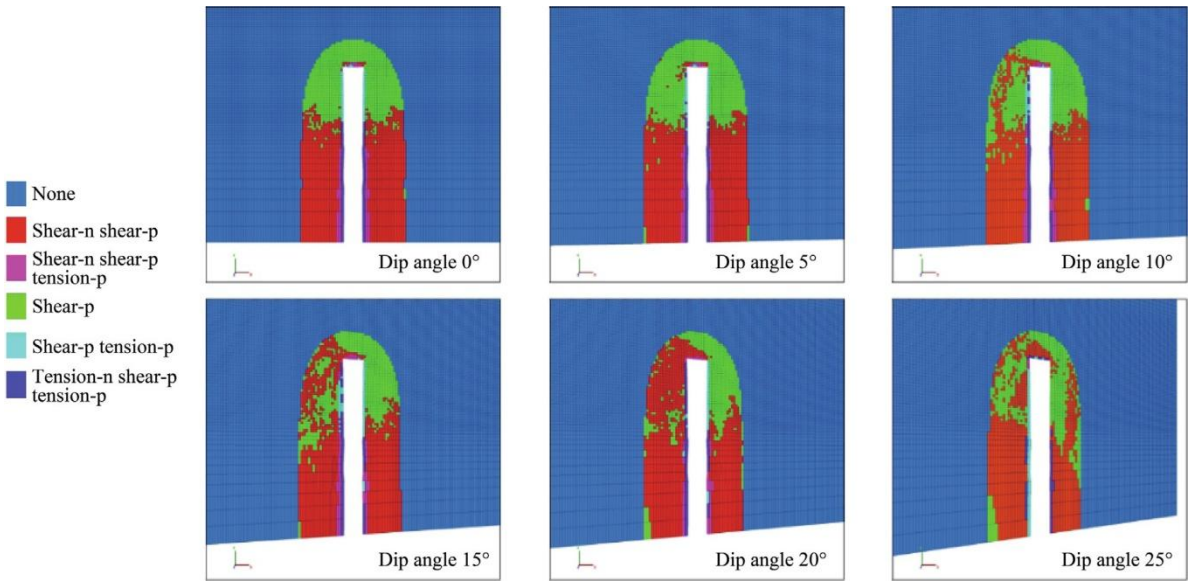

Fig. 7. Plastic zone in section plane of coal seam.

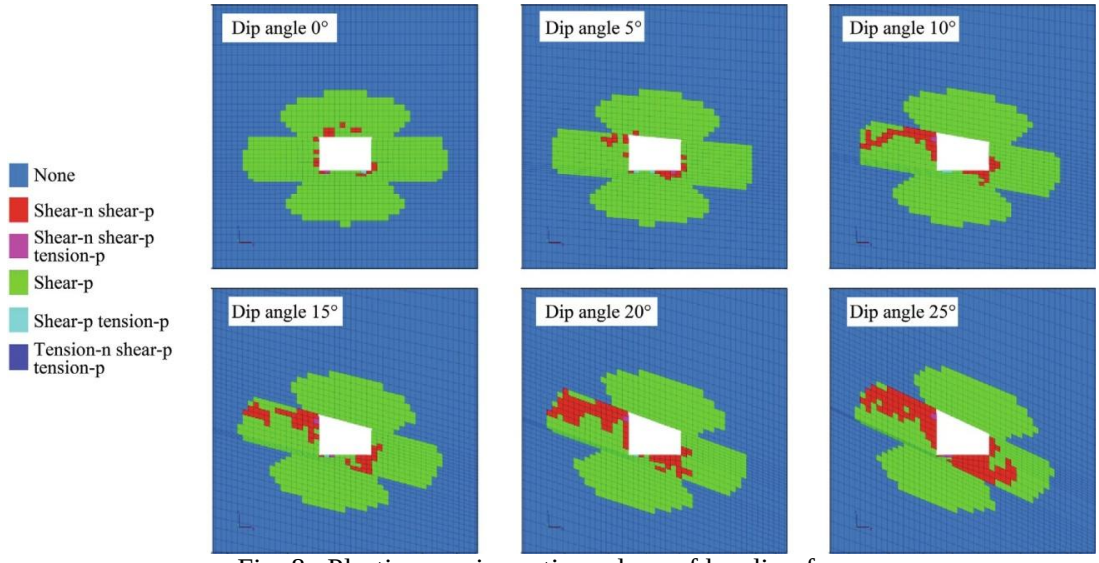

Fig. 8. Plastic zone in section plane of heading face.

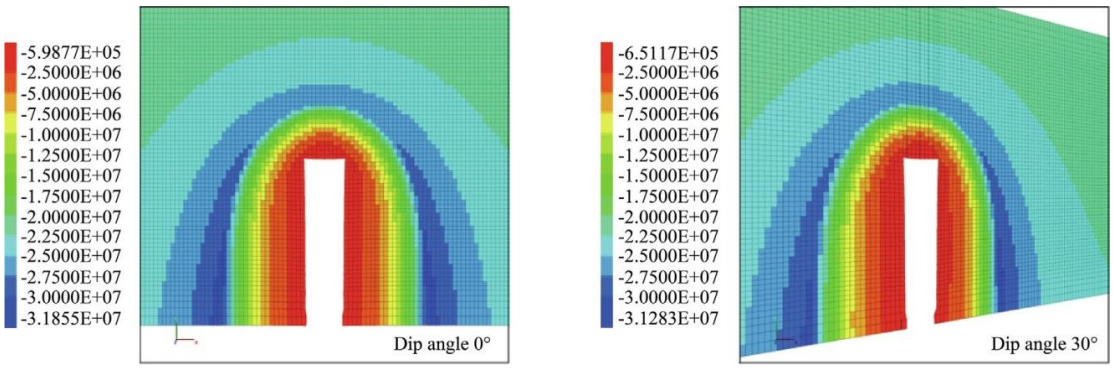

Fig. 9. Stress nephogram in section plane of coal seam.

points were arranged on each horizontal line, as exhibited in Fig. 1. Then the stress values were recorded and the horizontal stress curves were plotted, as presented in Fig. 10.

Fig. 10 demonstrates that the maximum principal stress of each measuring point generally increase with the rise of the distance from the heading face, while the increasing trend gradually declines. According to the estimation of curve variation trend, when the distance between a measuring point and the driving face exceeds 20 m, the stress changes slightly so that the stress state of coal seam tends to be in balance.

Displacement analysis of roadway surrounding rock

Fig. 11 is a displacement nephogram of coal seam profile. It can be observed from Fig. 11 that the displacement distribution of sur- rounding rock is a semi-elliptic multi-layer structure, and the dis- placement decreases gradually from the roadway to the outward. By analyzing the roadway wall area, it is found that the displace- ment of coal seam increases gradually along the roadway direction with the rise of distance from the driving face, which is consistent with the stress distribution.

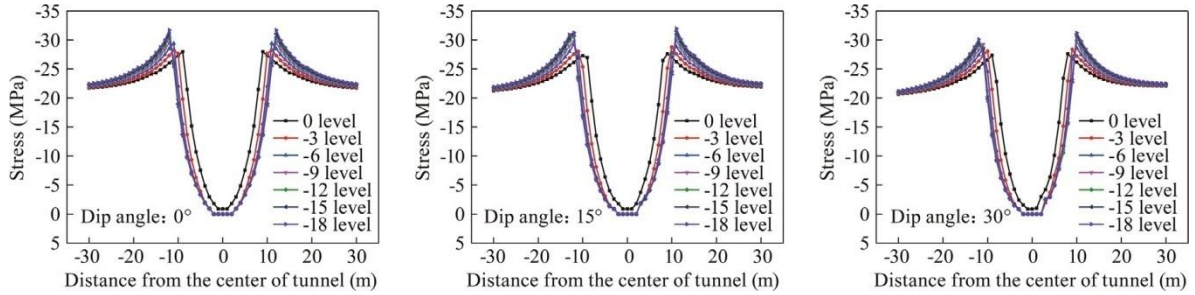

Fig. 10. Stress curve of measuring points in different levels.

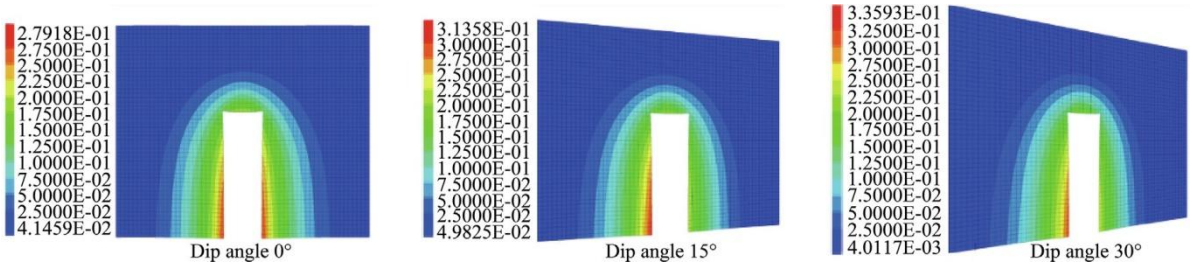

Fig. 11. Displacement nephogram in section plane of coal seam.

The roadway wall displacements at different distances from the driving face are recorded, as displayed in Fig. 12. Analysis of a sin- gle curve in Fig. 12 shows that the displacement curve of roadway wall presents an upward trend, and the increment of displacement is large near the driving face. However, it becomes smaller and smaller far away from the driving face, and the displacement curve gradually tends to level off. Comparison of displacement curves under different coal seam dip angle indicates that the displacement curves gradually climb with the increase of coal seam dip angle, that is, the displacement of roadway surrounding rock rise as a whole. By curve fitting, it is revealed that the displacement curves under all the coal seam dip angle tend to level off within the range of 18–25 m from the driving face. This means that balance is basi- cally restored around the roadway about 20 m away from the driv- ing face, but the distance for balance also increases with the rise of coal seam dip angle.

V. CONCLUSIONS

In this study, the outburst risk of driving face in the driving pro- cess was discussed by comparatively analyzing the stress distribu- tion, displacement distribution and plastic zone distribution of driving face under different coal seam dip angle. Besides, the range of unstable area of roadway surrounding rock during roadway driving was investigated through the comparison and analysis on the distribution law of stress and displacement in roadway sur- rounding rock under different coal seam dip angle. Based on the above research, the following conclusions were drawn:

(1) Regardless of the change of coal seam dip angle, the stress concentration area, displacement concentration area and plastic area are invariably located in the coal seam and the rock layer is relatively stable.

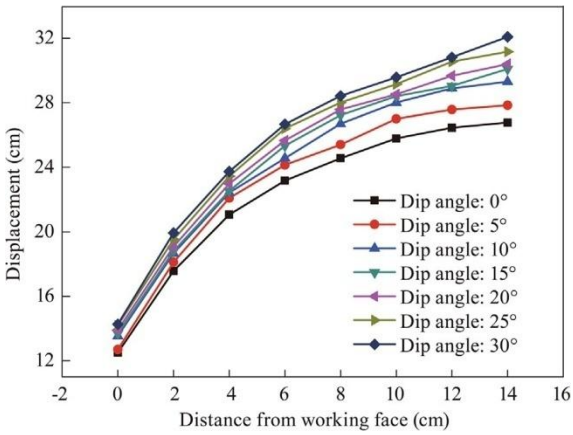

Fig. 12. Displacement curve of roadway wall.

(2) With the increase of coal seam dip angle, the risk of outburst around the heading face rises, and the area with high risk of outburst gradually moves upward along the coal seam.

(3) The unstable area of roadway surrounding rock concentrates near the driving face. With the increase of distance from the driving face, the instability of roadway surrounding rock gradually declines. At about 20 m away from the driving face, the roadway surrounding rock reaches balance. In addi- tion, the distance for balance goes up gradually with the increase of coal seam dip angle.

REFERENCES

[1]. Wang G, Chu X, Yang X. Numerical simulation of gas flow in artificial fracture coal by three-dimensional reconstruction based on computed tomography. J Nat Gas Sci Eng 2016;34:823–31.
[2]. Heidarzadeh S, Saeidi A, Rouleau A. Evaluation of the effect of geometrical parameters on stope probability of failure in the open stoping method using numerical modeling. Int J Min Sci Technol 2019;29(3):399–408.
[3]. Silva J, Worsey T, Lusk B. Practical assessment of rock damage due to blasting. Int J Min Sci Technol 2019;29(3):379–85.
[4]. Chen Z, Liu J, Pan Z, Connell LD, Elsworth D. Influence of the effective stress coefficient and sorption-induced strain on the evolution of coal permeability: model development and analysis. Int J Greenhouse Gas Control 2012;8:101–10.
[5]. Afum BO, Caverson D, Ben-Awuah E. A conceptual framework for characterizing mineralized waste rocks as future resource. Int J Min Sci Technol 2019;29(3):429–35.
[6]. Chu T, Li P, Chen Y. Risk assessment of gas control and spontaneous combustion of coal under gas drainage of an upper tunnel. Int J Min Sci Technol 2019;29(3):491–8.
[7]. Tang J, Pan Y, Yang S. Experimental study of coal and gas outburst under tridimensional stresses. Chinese J Rock Mech Eng 2013;05:960–5.
[8]. Ou J, Wang E, Xu W, Li Z. Study of the mechanism of coal and gas outburst induced by drilling. J China Univ Min Technol 2012;41(5):739–45.
[9]. Wang Z, Chen L, Sun L. Mechanism of delayed coal and gas outburst on working face in ‘‘three soft” mining areas. J China Univ Min Technol 2014;01:56–63.
[10]. Du J, Xu X, Li Z, Zhang X, Zhang H, Cao X. Rational control of driving speed in coal and gas outburst coal mining face. Coal Sci Technol 2013;12:43–5.
[11]. Zhang Y, Huang Z, Yu G, Zhang H. Coal and gas outbursts characteristics and countermeasures under the influence of geological conditions. Coal Sci Technol 2013;12:39–42.
[12]. Laubach SE, Marrett RA, Olson JE, Scott AR. Characteristics and origins of coal cleat: a review. Int J Coal Geol 1998;35(1):175–207.
[13]. Rodrigues CF, Laiginhas C, Fernandes M, Lemos De Sousa MJ, Dinis MAP. The coal cleat system: a new approach to its study. J Rock Mech Geotech Eng 2014;6(3):208–18.
[14]. Erdogan HH, Duzgun HS, Selcuk-Kestel AS. Quantitative hazard assessment for Zonguldak coal basin underground mines. Int J Min Sci Technol 2019;29 (3):453–67.
[15]. Santos TBD, Lana MS, Pereira TM, Canbulat I. Quantitative hazard assessment system (Has-Q) for open pit mine slopes. Int J Min Sci Technol 2019;29 (3):419–27.
[16]. Liu T, Lin B, Yang W, Zou Q, Kong J, Yan F. Cracking process and stress field evolution in specimen containing combined flaw under uniaxial compression. Rock Mech Rock Eng 2016;49(8):3095–113.
[17]. Cheng Y, Zhang X, Wang L. Controlling effect of ground stress on gas pressureand outburst disaster. J Min Saf Eng 2013;03:408–14.
[18]. Liu J, Xia H, Yang H, Wang Z. Comprehensive gas prevention and control technology of fully mechanized gateway driving face in seam with coal and gas outburst. Coal Sci and Technol 2012;04:67–70.
[19]. Fu J, Cheng Y. Situation of coal and gas outburst in china and control countermeasures. J Min Saf Eng 2007;03:253–9.
[20]. Hu Q, Zhao X. Present situation of coal and gas outburst accidents in china’s coal mines and countermeasures and suggestions for their prevention. Min Saf Environ Prot 2012;05:1–6.
[21]. Hossain MM, Rahman MK. Numerical simulation of complex fracture growth during tight reservoir stimulation by hydraulic fracturing. J Petrol Sci Eng 2008;60(2):86–104.
[22]. Ni GH, Lin BQ, Zhai C. Impact of the geological structure on pulsating hydraulic fracturing. Arab J Geosci 2015;8(12):10381–8.

[23]. Zhai C, Xu JZ, Liu S, Qin L. Fracturing mechanism of coal-like rock specimens under the effect of non-explosive expansion. Int J Rock Mech Min Sci 2018;103:145–54.
[24]. Zhou G, Zhang Q, Bai R, Fan T, Wang G. The diffusion behavior law of respirable dust at fully mechanized caving face in coal mine: CFD numerical simulation and engineering application. Process Saf Environ Prot 2017;106:117–28.
[25]. Wang G, Li W, Wang P, Yang X, Zhang S. Deformation and gas flow characteristics of coal-like materials under triaxial stress conditions. Int J Rock Mech Min Sci 2017;91:72–80.
[26]. Wang H, Nie W, Cheng W, Liu Q, Jin H. Effects of air volume ratio parameters on air curtain dust suppression in a rock tunnel's fully-mechanized working face. Adv Powder Technol 2018;29(2):230–44.
[27]. Sampath KHSM, Perera MSA, Elsworth D, Ranjith PG, Matthai SK, Rathnaweera T, et al. Effect of coal maturity on CO_2-based hydraulic fracturing process in coal seam gas reservoirs. Fuel 2019;236:179–89.
[28]. Yan F, Lin B, Zhu C, Zhou Y, Liu X, Guo C, et al. Experimental investigation on anthracite coal fragmentation by high-voltage electrical pulses in the air condition: effect of breakdown voltage. Fuel 2016;183:583–92.
[29]. Fan T, Zhou G, Wang J. Preparation and characterization of a wetting- agglomeration-based hybrid coal dust suppressant. Process Saf Environ Prot 2018;113:282–91.
[30]. Kong B, Wang E, Li Z. The effect of high temperature environment on rock properties-an example of electromagnetic radiation characterization. Environ Sci Pollut Res 2018;25(29):29104–14.
[31]. Rageh OS, Koraim AS. Hydraulic performance of vertical walls with horizontal slots used as breakwater. Coast Eng 2010;57(8):745–56.
[32]. Devloo PRB, Fernandes PD, Gomes SM, Bravo CMAA, Damas RG. A finite element model for three dimensional hydraulic fracturing. Math Comput Simul 2006;73(1–4):142–55.
[33]. Klammler H, Nemer B, Hatfield K. Effect of injection screen slot geometry on hydraulic conductivity tests. J Hydrol 2014;511:190–8.
[34]. Wang E, Li Z, He X, Chen L. Application and pre-warning technology of coal and gas outburst by electromagnetic radiation. Coal Sci Technol 2014;06:53–7.
[35]. Jiang F, Yin Y, Zhu Q, Wang C, Qu X. Experimental study of precaution technology of heading face coal and gas outburst based on dynamic changes of stress and methane concentration. Chinese J Rock Mech Eng 2014;S2:3581–8.
[36]. Shu L, Wang K, Qi Q, Zhang L. Stress field evolution characteristics and coal-gas outburst hazard evaluation model of the heading face in coal roadway. J Min Saf Eng 2017;02:259–67.
[37]. Guo Z, Zhao G, Peng K. Study on wallrock deformation by FLAC3D simulation of excavation and support in deep high-stress soft-rock roadway. Min Metall Eng 2012;02:18–22.
[38]. Li H, Lin B, Yang W, Gao Y, Liu T. Effects of an underlying drainage gallery on coal bed methane capture effectiveness and the mechanical behavior of a gate road. J Nat Gas Sci Eng 2015;27:616–31.
[39]. Jiao H, Yang S, Li H. Study on numerical simulations of outburst risk influence on cross cut in uncovering coal seam at different dip angles. Coal Technol 2015;04:150–3.
[40]. Yang W. Mechanical Behavior Evolution of Mining Stope and Gas Control Technolog. Xuzhou: China University of Mining and Technology; 2013.
[41]. Liu T, Lin BQ, Zou QL, Zhu C, Yan FZ. Mechanical behaviors and failure processes of precracked specimens under uniaxial compression: a perspective from microscopic displacement patterns. Tectonophysics 2016;672– 673:104–20.